

Gagnon, C.A., Butler, K.L., Gaviria, E., Terrazas, A., Gao, A., Bhattacharya, T., Boutt, D.F., Munk, L.A., and Ibarra, D.E., 2023, Title: GSA Bulletin, <https://doi.org/10.1130/B36572.1>.

Supplemental Material

Figure S1. Age Model with Halite Slumps.

Figure S2. EXP2 Time series with weathering indices.

Figure S3. CIA ternary diagram.

Table S1. EXP2 age constraints.

Table S2. EXP2 samples and data table.

Table S3. Zircon U-Pb data.

Table S4. $^{40}\text{Ar}/^{39}\text{Ar}$ data.

Table S5. Fish Lake Valley age constraints.

Table S6. Fish Lake Valley samples and data table **Table S7.** Modern water samples.

SUPPLEMENTARY MATERIALS

for

Paleoclimate controls on lithium enrichment in Great Basin

Pliocene-Pleistocene lacustrine clays

Catherine A. Gagnon^{1,2,†}, Kristina L. Butler³, Elizabeth Gaviria^{1,4}, Alexa Terrazas⁵, Annabelle Gao¹, Tripti Bhattacharya⁶, David F. Boutt⁷, Lee Ann Munk⁸, Daniel E. Ibarra^{1,2}

¹*Department of Earth, Environmental and Planetary Science, Brown University, Providence, RI 02912, USA*

²*Institute at Brown for Environment and Society, Brown University, Providence, RI 02912, USA*

³*Department of Geological Sciences, Jackson School of Geosciences, University of Texas at Austin, Austin, TX 78712, USA*

⁴*Department of Earth, Environmental and Planetary Sciences, Rice University, Houston, TX 77005, USA*

⁵*Department of Ocean and Atmospheric Sciences, University of California, Los Angeles, CA, 90095, USA*

⁶*Department of Earth Sciences, Syracuse University, Syracuse, NY 12344, USA*

⁷*Department of Geosciences, University of Massachusetts-Amherst, Amherst, MA 01003, USA*

⁸*Department of Geological Sciences, University of Alaska Anchorage, Anchorage, AK 99508, USA*

† Corresponding author: catherine_gagnon@brown.edu

The following is included in this file:

Figure S1. Age Model with Halite Slumps

Figure S2. EXP2 Time series with weathering indices

Figure S3. CIA ternary diagram

The following is included in an attached Excel File:

Table S1. EXP2 age constraints

Table S2. EXP2 samples and data table

Table S3. Zircon U-Pb data

Table S4. $^{40}\text{Ar}/^{39}\text{Ar}$ data

Table S5. Fish Lake Valley age constraints

Table S6. Fish Lake Valley samples and data table

Table S7. Modern water samples

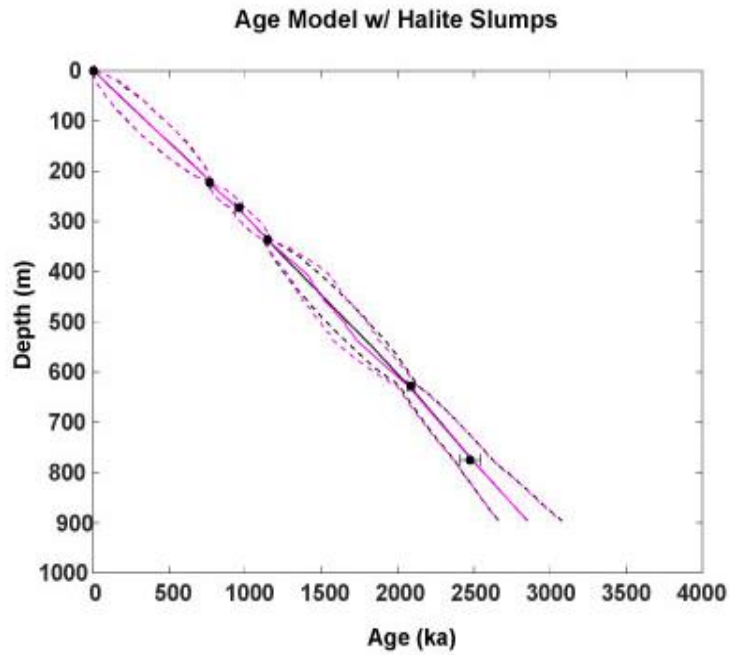


Fig S1. Bacon age-depth model using ash slumps only (black) and added halite slumps (magenta). Age control points are the same as Fig 1.

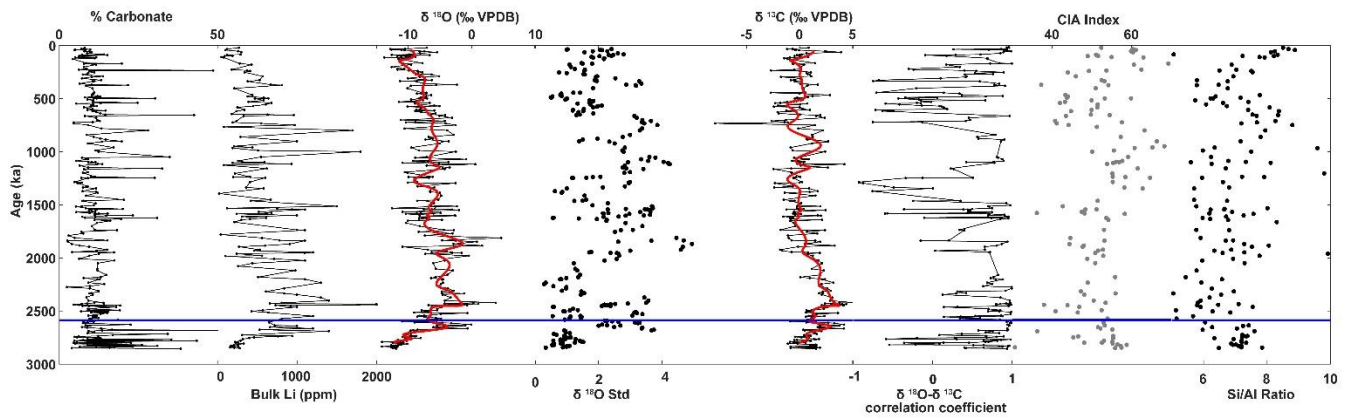


Figure S2. Full time series from the Clayton Valley EXP2. From left to right: percent carbonate; bulk sediment lithium concentrations (ppm); carbonate $\delta^{18}\text{O}$ (‰ VPDB); 5 point running carbonate $\delta^{18}\text{O}$ standard deviation; carbonate $\delta^{13}\text{C}$ (‰ VPDB); correlation coefficient between oxygen and carbon isotopes with a moving window of 10 data points; chemical index of alteration; and Si/Al ratio. Solid red lines are a low pass filtered curve on the carbonate $\delta^{18}\text{O}$ and $\delta^{13}\text{C}$ records.

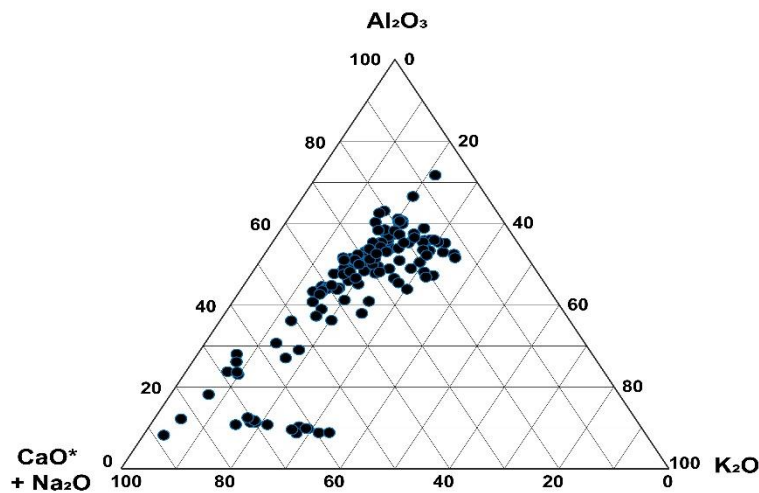


Figure S3. Ternary diagram for all clay samples with available data, showing the relative mole fractions of CaO+Na₂O, K₂O, and Al₂O₃.

Weathering Indices

The results of the CIA calculations are summarized in Figure S2 and shown in the time series in Figure S3. There does not appear to be a distinction between the lithologies in terms of the CIA values, with most plotting close to the Ca/Na and Al endmembers. There are, however, distinct shifts in the CIA value time series (Figure S3). From the base of the core, the CIA values stay below 40 until they reach the top of the halite beds where they then increase their weathered CIA value to ~60. The weathering indices stay high until the base of the thick ash at ~750 ka where they drop to below 40. From the base of the ash to the top of the core the CIA values then increase gradually. We also plot Si/Al on Figure S3, which shows similar trends.